Supporting Information for

Synthesis of Zeolite@Mesoporous Silica Composite to Improve Low-frequency Acoustic Performance of Miniature Loudspeaker System

Kongxin Liu [a], Yifei Zeng [a], Lu Han *[a] and Shunai Che*[a,b]

a. School of Chemical Science and Engineering, Tongji University, Shanghai 200092, P. R. China

b. School of Chemistry and Chemical Engineering, Frontiers Science Center for Transformative Molecules, State Key Laboratory of Matrix Composite, Shanghai Key Laboratory for Molecular Engineering of Chiral Drugs, Shanghai Jiao Tong University, 800 Dongchuan Road, Shanghai, 200240 P. R. China

Corresponding Author: Lu Han: luhan@tongji.edu.cn, Shunai Che: chesa@sjtu.edu.cn

1. Synthesis

Synthesis of imporous sample. The imporous material was synthesized as the same way of synthesizing Z@MS, but without adding surfactant and zeolites. Other steps and operation were constant.

Synthesis of MSU. The pure mesoporous material (MSU) was synthesized as the same way of synthesizing Z@MS, but without adding zeolites. Other steps and operation were constant.

Synthesis of microporous sample. The microporous material was synthesized by binding raw zeolite grains with silica sol to acquire a monolithic morphology. 10 g

zeolites were added in 12 g silica sol (Kehan New Materials (Shandong) Co., Ltd., KHZ8040) and 2 g water, and the suspension was stirred at room temperature for 12 h. Then, the suspension was centrifuged to collect sediment. Afterwards, it was washed, dried, and calcined (5 ℃/min) at 550 ℃ for 6 h.

Synthesis of Z@MS with different framework. The different framework Z@MS was synthesized as the same way of synthesizing Z@MS containing MFI zeolite. In the process, BEA, MOR, and TON zeolite of equal weight are respectively used to replace MFI.

Synthesis of Z@MS by polyoxyl stearyl ether of different degree of polymerization. This is the same route as using PEO surfactant, Brij 72 ($C_{18}H_{37}(OCH_2CH_2)_2OH$) to synthesize Z@MS as in our manuscript. The only variable was the use of polyoxyl stearyl ether with different degrees of 2, 7, 10, and 50, instead of Brij 72.

2. Acoustic measurement of miniature loudspeaker system.

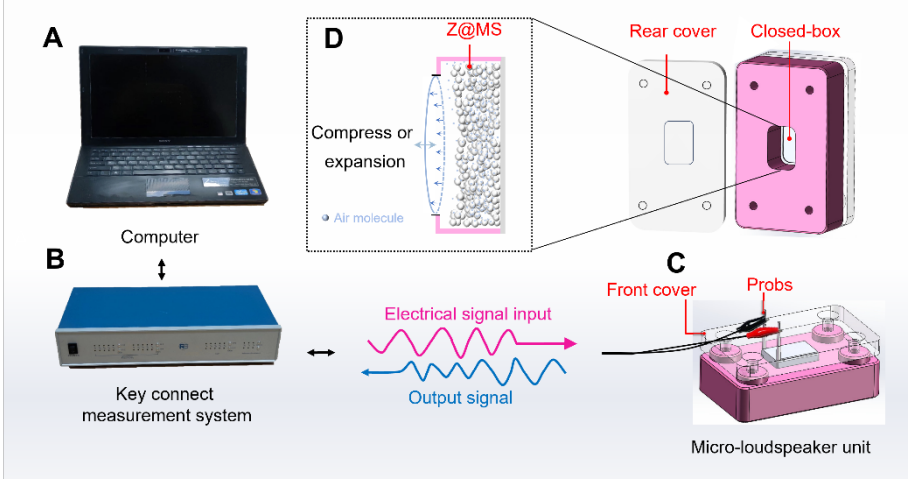

Figure S1. The platform for acoustic measurement.

Firstly, the Trustsystem 10.0 (one software by Beijing RStech) in the computer (Figure S1A) is programmed with specific parameters (impedance: 8±10% ohms@2kHz, start Hz: 100, stop Hz: 1600, points:300) and then electrical signals are input into micro-loudspeaker unit (Figure S1C) by the Key connect measurement system (Figure S1B). Then, the micro-loudspeaker unit receive signal, sound, and return the output signal to the Key connect measurement system. During the sound process, the compression and expansion of the diaphragm drive air molecules and interact with Z@MS in a fully sealed closed-box with 1.0 cc volume.

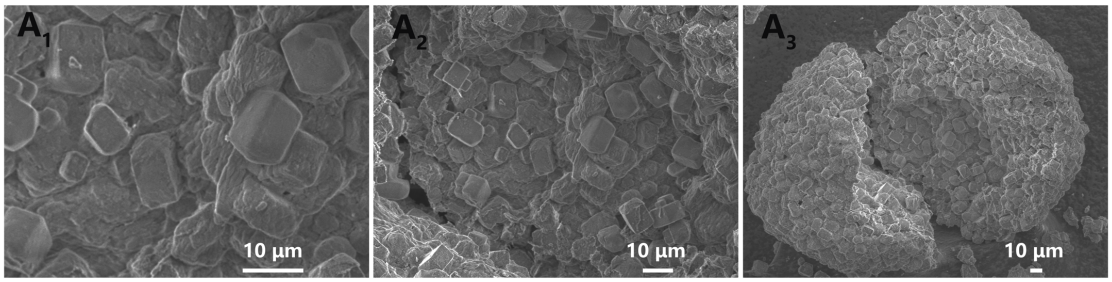

Figure S2. SEM images of internal cross-section of Z@MS particle.

2. Characterization

Table S1. Summary of the physical properties of raw MFI zeolite and Z@MS shown in Figure 1.

Material	S_{BET}[a]/($m^2 \cdot g^{-1}$)	V_p[b]/($cm^3\ g^{-1}$)	$V_{t\text{-}plot}$[c]/($cm^3\ g^{-1}$)
MFI	387.6	0.20	0.173
Z@MS	360.4	0.25	0.116

a. BET specific surface area(p/p_0=0.05-0.35); b. total pore volume; c. t-plot micropore volume calculated on the basis of N_2-sorption isotherms.

Table S2. Resonance frequency (f_0) measurement results of Z@MS with different loading volume shown in Figure 3.

Loading volume/cc	f_0/Hz	f_0'/Hz	Δf_0/Hz
0.25	885.63	816.08	69.55
0.50	885.63	721.85	163.78
0.75	885.63	600.51	285.12
1.00	885.63	545.86	339.77

f_0: the resonance frequency of empty chamber; f_0': the resonance frequency after filling with sample; Δf_0: reduced value of f_0.

Table S3. Resonance frequency (f_0) measurement results of Z@MS with different particle size range shown in Figure 4.

Particle size range/μm	f_0/Hz	f_0'/Hz	Δf_0/Hz
150-154	885.63	545.86	339.77
154-180	885.63	564.78	320.85
180-224	885.63	592.38	293.25
224-355	885.63	674.29	211.34

f_0: the resonance frequency of empty chamber; f_0': the resonance frequency after filling with sample; Δf_0: reduced value of f_0.

Table S4. Summary of the physical properties of imporous, MSU, microporous material and Z@MS shown in Figure 6.

Material	S_{BET}[a]/($m^2 \cdot g^{-1}$)	V_p[b]/($cm^3\ g^{-1}$)	$V_{t\text{-}plot}$[c]/($cm^3\ g^{-1}$)
imporous	5.3	0.00	0.000
MSU	473.7	0.74	0.000
microporous	232.6	0.15	0.090
Z@MS	360.4	0.25	0.116

a. BET specific surface area(p/p_0=0.05-0.35); b. total pore volume; c. t-plot micropore volume calculated on the basis of N_2-sorption isotherms.

Table S5. Resonance frequency (f_0) measurement results of imporous, MSU, microporous material and Z@MS shown in Figure 6.

Material	f_0/Hz	f_0'/Hz	Δf_0/Hz
imporous	891.69	904.37	-12.68
MSU	891.69	745.49	146.20
microporous	891.69	660.64	231.05
Z@MS	891.69	568.65	323.04

f_0: the resonance frequency of empty chamber; f_0': the resonance frequency after filling with sample; Δf_0: reduced value of f_0.

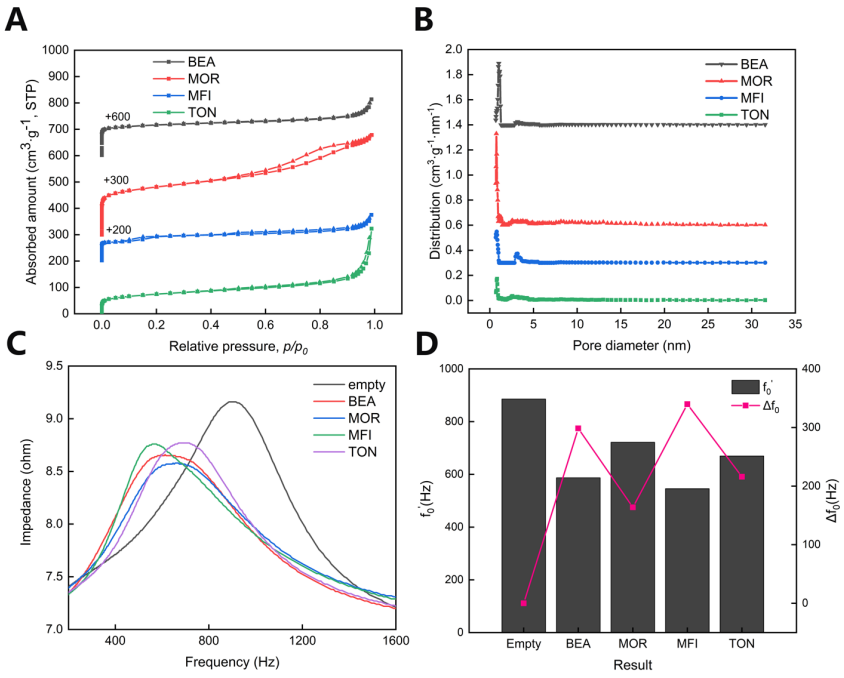

Figure S3. Pore structural characteristics and acoustic performance of Z@MS samples synthesized by zeolites of different frameworks. (A) Adsorption and desorption isotherm of N_2 at 77 K. (B) Pore size distribution calculated by NLDFT. (C) Impedance-frequency curves. (D) Resonance frequency and corresponding offsets.

Table S6. Resonance frequency (f_0) measurement results of Z@MS samples synthesized by zeolites of different frameworks shown in Figure S3.

Framework type	f_0/Hz	f_0'/Hz	Δf_0/Hz
BEA	885.63	587.14	298.49
MOR	885.63	721.85	163.78
MFI	885.63	545.86	339.77
TON	885.63	669.71	215.92

f_0: the resonance frequency of empty chamber; f_0': the resonance frequency after filling with sample; Δf_0: reduced value of f_0.

Table S7. Summary of the physical properties of Z@MS samples synthesized by zeolites of different frameworks shown in Figure S3.

Framework type	S_{BET}[a]/($m^2 \cdot g^{-1}$)	V_p[b]/($cm^3\ g^{-1}$)	$V_{t\text{-}plot}$[c]/($cm^3\ g^{-1}$)
BEA	264.9	0.22	0.16
MOR	661.4	0.52	0.16
MFI	316.9	0.20	0.13
TON	264.9	0.21	0.07

a. BET specific surface area(p/p_0=0.05-0.35); b. total pore volume; c. t-plot micropore volume calculated on the basis of N_2-sorption isotherms.

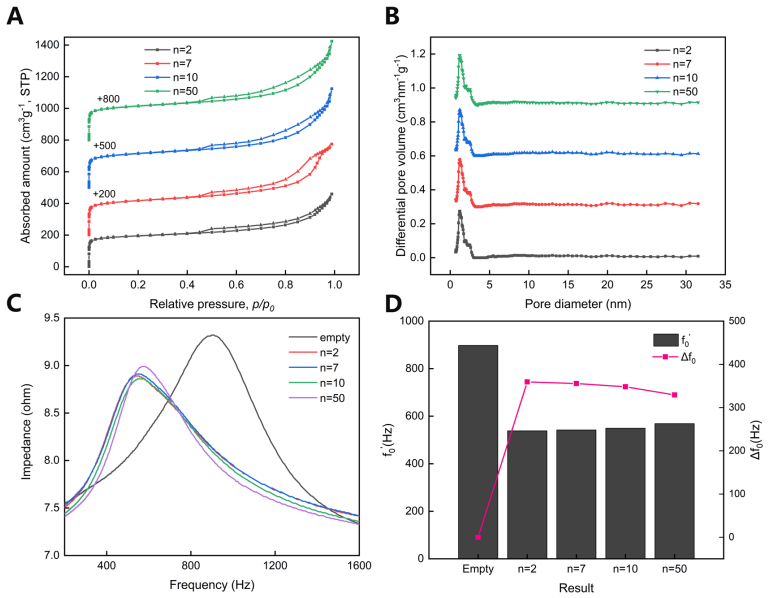

Figure S4. Pore structural characteristics and acoustic performance of Z@MS samples synthesized by polyoxyl stearyl ether of different degree of polymerization. (A) Adsorption and desorption isotherm of N_2 at 77 K. (B) Pore size distribution calculated by NLDFT. (C) Impedance-frequency curves. (D) Resonance frequency and corresponding offsets.

Table S8. Resonance frequency (f_0) measurement results of Z@MS samples synthesized by polyoxyl stearyl ether of different degree of polymerization shown in Figure S4.

Polymerization degree	f_0/Hz	f_0'/Hz	Δf_0/Hz
n=2	897.79	538.47	359.32
n=7	897.79	542.15	355.64
n=10	897.79	549.59	348.2
n=50	897.79	568.65	329.14

f_0: the resonance frequency of empty chamber; f_0': the resonance frequency after filling with sample; Δf_0: reduced value of f_0.

Table S9. Summary of the physical properties of Z@MS samples synthesized by polyoxyl stearyl ether of different degree of polymerization shown in Figure S4.

Polymerization degree	S_{BET}[a]/($m^2 \cdot g^{-1}$)	V_p[b]/($cm^3\ g^{-1}$)	$V_{t\text{-}plot}$[c]/($cm^3\ g^{-1}$)
n=2	750.4	0.49	0.23
n=7	820.9	0.64	0.24
n=10	809.0	0.64	0.24
n=50	883.7	0.63	0.25

a. BET specific surface area(p/p_0=0.05-0.35); b. total pore volume; c. t-plot micropore volume calculated on the basis of N_2-sorption isotherms.